

Session 2
Dynamos and Cycle Variability

Cycles and cycle modulations

Axel Brandenburg^{1,2} and Gustavo Guerrero^{1,3}

¹Nordita, Roslagstullsbacken 23, SE-10691 Stockholm, Sweden
email: brandenb@nordita.org

²Department of Astronomy, Stockholm University, SE-10691 Stockholm, Sweden

³Solar Physics, HEPL, Stanford University, Stanford, CA 94305-4085, USA

Abstract. Some selected concepts of the solar activity cycle are reviewed. Cycle modulations through a stochastic α effect are being identified with limited scale separation ratios. Three-dimensional turbulence simulations with helicity and shear are compared at two different scale separation ratios. In both cases the level of fluctuations shows relatively little variation with the dynamo cycle. Prospects for a shallow origin of sunspots are discussed in terms of the negative effective magnetic pressure instability. Tilt angles of bipolar active regions are discussed as a consequence of shear rather than the Coriolis force.

Keywords. MHD, turbulence, Sun: activity, Sun: magnetic fields, sunspots

1. Solar cycle

The solar cycle manifests itself through spots at the Sun's surface. To understand activity variations, we have to understand not only their source, but also the detailed connection between variations in the strength of the dynamo and its effect on the number and size of sunspots. In this paper, we address both aspects.

The physics of the solar cycle is not entirely clear. The models that work best are not necessarily those that would emerge from first principles. Even the reason for the equatorward migration of the activity belts is not completely clear. Following Parker's seminal paper of 1955, this migration seemed to be a simple property of an $\alpha\Omega$ dynamo, i.e., a dynamo that works with α effect and shear. What matters for equatorward migration is not the Ω gradient in the latitudinal direction, but that in the radial one, $\partial\Omega/\partial r$. However, in the bulk of the convection zone, $\partial\Omega/\partial r$ is mostly positive. This, together with an α effect of positive sign in the northern hemisphere results in poleward migration (Yoshimura 1975), which is not what is observed. On the other hand, according to the flux transport dynamos, magnetic fields are advected by the meridional circulation. Assuming that there is a coherent circulation with equatorward migration at the bottom of the convection zone, this would then turn the dynamo wave around so as to explain the solar butterfly diagram and that sunspots emerge from progressively lower latitudes (Choudhuri *et al.* 1995; Dikpati & Charbonneau 1999; Guerrero & de Gouveia Dal Pino 2008). This requires that most of the field resides at the bottom of the convection zone. Moreover, the α effect is taken to be non-vanishing only near the very top of the convection zone, i.e., the mean electromotive force has to be written formally as a convolution of the mean magnetic field with an integral kernel to account for this non-locality (see, e.g., Brandenburg & Käpylä 2007). Furthermore, from the observed tilt angles of bipolar regions it is inferred that the Sun's magnetic field at the bottom of the convection zone reaches strengths of the order of 100 kG (D'Silva & Choudhuri 1993), which is nearly 100 times over the equipartition value. Finally, there are assumptions about the turbulent magnetic diffusivity. In all cases, the magnetic diffusivity in the evolution equation for

the toroidal field in the bulk of the convection zone is rather small, below $10^{11} \text{ cm}^2 \text{ s}^{-1}$ (see, e.g., Chatterjee & Choudhuri 2006). The magnetic diffusivity for the poloidal field is assumed to be larger and similar to the values expected from mixing length theory (see below).

In any case, these assumptions are hardly in agreement with standard formulae that the magnetic diffusivity is given by $\frac{1}{3}\tau u_{\text{rms}}^2$, where τ is the turnover time and u_{rms} is the rms value of the turbulent velocity. The turnover time is $\tau = (u_{\text{rms}} k_f)^{-1}$, where k_f is the wavenumber of the energy-carrying eddies. This result for η_t is well confirmed by simulations (Sur *et al.* 2008). For the Sun, mixing length theory appears to be reasonably good and gives $\eta_t \approx (1...3) \times 10^{12} \text{ cm}^2 \text{ s}^{-1}$. Also, in contrast to the assumptions of some flux transport dynamo models, a strong degree of anisotropy of the η tensor is not expected from theory (Brandenburg *et al.* 2012).

An alternate approach is to use turbulent transport coefficients from theory, which give rise to what is called a distributed dynamo, i.e., the induction effects are non-vanishing and distributed over the entire convection zone. In addition, there is the hypothesis that the near-surface shear layer may be important for the equatorward migration (Brandenburg 2005), but this has never been confirmed by simulations either. In any case, based on such models one would not expect there to be a 100 kG magnetic field, but only a much weaker field of around 0.3–1 kG. This calls then for an alternative explanation for the magnetic field concentrations of up to 3 kG seen in sunspots and active regions. Various proposals were already discussed in Brandenburg (2005), and meanwhile there are direct numerical simulations (DNS) confirming the validity of the physics assumed in one of those proposals. This will be addressed in Section 3.

2. Cycle modulation

Early ideas for cycle modulations go back to Tavakol (1978) who argued that the solar cycle may be a chaotic attractor. This explanation became very popular in the following years (Ruzmaikin 1981; Weiss *et al.* 1984). These ideas were elaborated upon in the framework of low-order truncations of mean-field dynamo models, having in mind that the same idea applies also to the underlying fully nonlinear three-dimensional equations of magnetohydrodynamics. Another line of thinking is that in mean-field theory (MFT) the physics of the cycle models can be explained by random fluctuations in the turbulent transport coefficients (Choudhuri *et al.* 1992; Moss *et al.* 1992; Schmitt *et al.* 1996; Brandenburg & Spiegel 2008). For high-dimensional attractors there is hardly any difference between both approaches. A completely different proposal for cycle modulation is related to variations in the meridional circulation (Nandy *et al.* 2011). This proposal still lacks verification from DNS of a dynamo whose cycle period is indeed controlled by meridional circulation. By contrast, fluctuations in the turbulent transport coefficients have indeed been borne out by simulations (see Brandenburg *et al.* 2008).

To illustrate this, let us now consider a physical realization of a simple $\alpha\Omega$ dynamo in a periodic domain. In the language of MFT, this corresponds to solving the following set of mean-field equations,

$$\frac{\partial \bar{\mathbf{B}}}{\partial t} = \nabla \times (\bar{\mathbf{U}} \times \bar{\mathbf{B}} + \bar{\boldsymbol{\varepsilon}} - \eta \mu_0 \bar{\mathbf{J}}) \quad (2.1)$$

in a Cartesian domain, (x, y, z) , in one dimension, $-\pi < z < \pi$, where $\bar{\mathbf{U}} = \bar{U}_S \equiv (0, Sx, 0)$ is a linear shear flow velocity (assuming $S = \text{const}$), $\bar{\mathbf{J}} = \nabla \times \bar{\mathbf{B}}/\mu_0$ is the mean current density, μ_0 is the vacuum permeability, η is the microphysical (molecular)

magnetic diffusivity, and

$$\bar{\mathcal{E}} = \alpha \bar{\mathbf{B}} - \eta_t \mu_0 \bar{\mathbf{J}} \tag{2.2}$$

is the mean electromotive force. In DNS, on the other hand, one solves directly the equation

$$\frac{\partial \mathbf{B}}{\partial t} = \nabla \times (\mathbf{U} \times \mathbf{B} - \eta \mu_0 \mathbf{J}), \tag{2.3}$$

together with corresponding equations governing the evolution of the turbulent velocity \mathbf{U} . Here, one often make the assumption of an isothermal gas with constant sound speed c_s . This will also be done in the present work.

In the following we present results of simulations using shearing–periodic boundary conditions. To maintain the solenoidality of the magnetic field, we write $\mathbf{B} = \nabla \times \mathbf{A}$ and solve for the magnetic vector potential \mathbf{A} . Using in the following the velocity for the deviations from the shear flow, \mathbf{U} , our equations are

$$\frac{\partial \mathbf{A}}{\partial t} + \mathbf{U}_S \cdot \nabla \mathbf{A} = -S A_y \mathbf{x} + \mathbf{U} \times \mathbf{B} + \eta \nabla^2 \mathbf{A}, \tag{2.4}$$

$$\frac{\mathcal{D} \mathbf{U}}{\mathcal{D} t} = -S U_x \mathbf{y} - c_s^2 \nabla \ln \rho + \mathbf{f} + \frac{1}{\rho} (\mathbf{J} \times \mathbf{B} + \nabla \cdot 2\nu \rho \mathbf{S}), \tag{2.5}$$

$$\frac{\mathcal{D} \ln \rho}{\mathcal{D} t} = -\nabla \cdot \mathbf{U}, \tag{2.6}$$

where $\mathcal{D}/\mathcal{D}t = \partial/\partial t + (\mathbf{U} + \mathbf{U}_S) \cdot \nabla$ is the advective derivative with respect to the total flow, $\mathbf{U} + \mathbf{U}_S$, ρ is the gas density, ν is the viscosity, $S_{ij} = \frac{1}{2}(U_{i,j} + U_{j,i}) - \frac{1}{3}\delta_{ij} \nabla \cdot \mathbf{U}$ is the trace-less rate of strain matrix, and \mathbf{f} is a forcing function that drives both turbulence and a linear shear flow. Alternatively, turbulence can also be the result of some instability (Rayleigh–Bénard instability, magneto-rotational instability, etc). In the following we restrict ourselves to a random forcing function with wavevectors whose modulus is in a narrow interval around an average wavenumber k_f . This has the additional advantage that we can arrange the forcing function such that it has a part that is fully helical, i.e., $\nabla \times \mathbf{f} = k_f \mathbf{f}$ (the part driving the shear flow is of course non-helical). Because of the presence of helicity, we should expect there to be an α effect operating in the system, but if the number of turbulent eddies in the domain is not very large, there can be significant fluctuations in the resulting α effect.

Important control parameters are the magnetic Reynolds and Prandtl numbers, $\text{Re}_M = u_{\text{rms}}/\eta k_f$ and $\text{Pr}_M = \nu/\eta$. In addition, there is the non-dimensional shear parameter defined here as $\text{Sh} = S/u_{\text{rms}} k_f$. The smallest possible wavenumber in a triply-periodic domain of size $L \times L \times L$ is $k_1 = 2\pi/L$. For the purpose of presenting exploratory results, we restrict ourselves here to a resolution of 64^3 meshpoints. We use the fully compressible PENCIL CODE† for all our calculations.

In Figure 1 we present the results of two simulations with scale separation ratios k_f/k_1 of 1.5 and 2.2. In both cases, k_f/k_1 is still relatively small, but the difference in the results is already quite dramatic. For $k_f/k_1 = 2.2$ the cycle is more regular while for 1.5 it is quite erratic. We show the toroidal field (i.e. the component B_y in the direction of the mean shear flow) at an arbitrarily chosen mesh point as well as its squared value (which could be taken as a proxy of the sunspot number), the mean magnetic energy in the full domain, as well as its contributions from the mean and fluctuating fields. In all cases, the magnetic field is normalized by the equipartition value, $B_{\text{eq}} = \sqrt{\mu_0 \rho_0} u_{\text{rms}}$, where $\rho_0 = \langle \rho \rangle$ is the mean density, which is conserved for periodic and shearing–periodic boundary conditions.

† <http://www.pencil-code.googlecode.com>

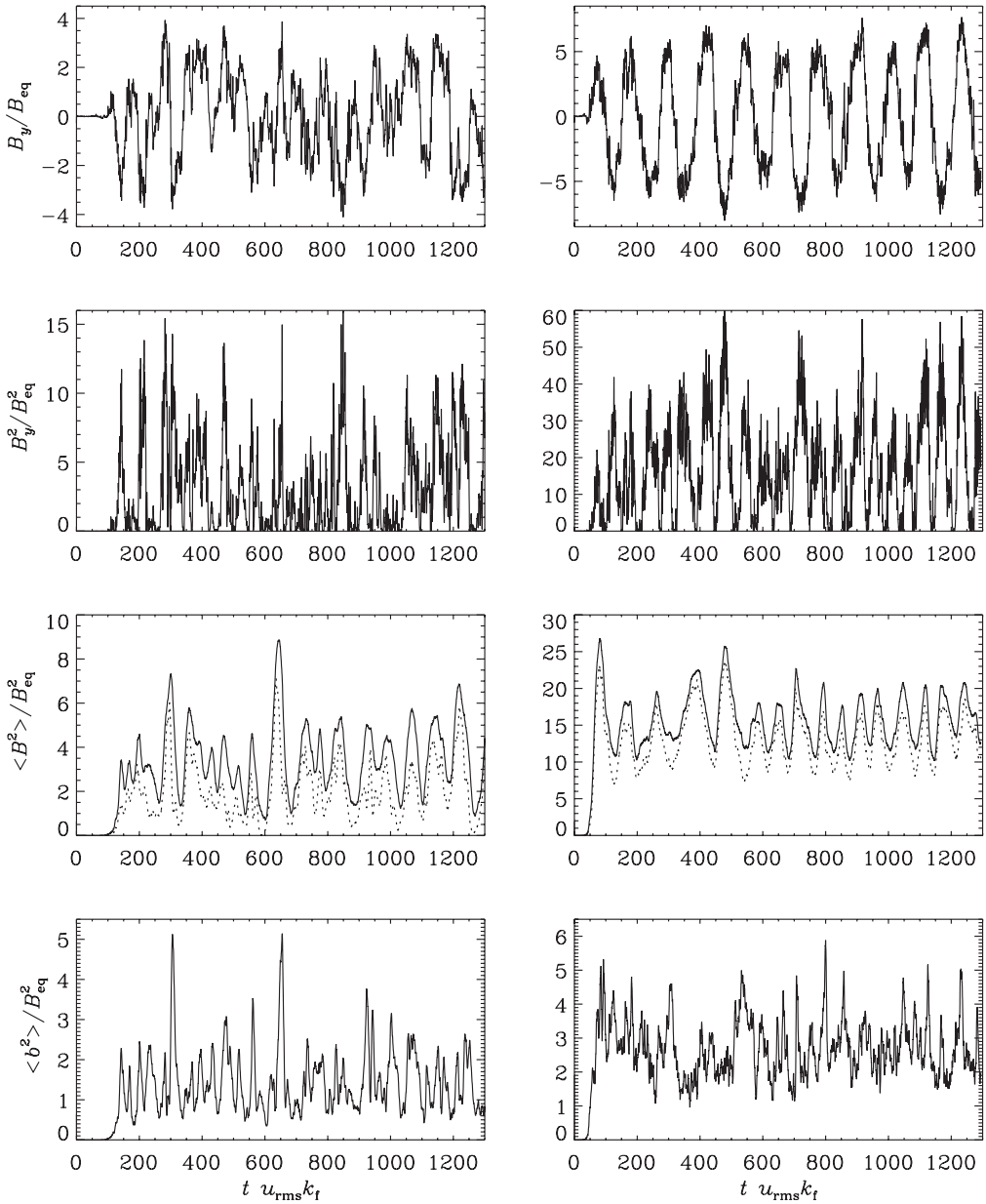


Figure 1. Time sequences of B_y , B_y^2 , $\langle B^2 \rangle$ (solid line) together with $\overline{B^2}$ (dotted line), and $\langle b^2 \rangle$. The field is always normalized by B_{eq} . Here, $Re_M = 22$ for $k_t/k_1 = 1.5$ (left column) and $Re_M = 9$ for $k_t/k_1 = 2.2$ (right column). In both cases, $Pr_M = 5$ and $Sh \approx -2$.

Here, angle brackets denote volume averages and overbars are defined as xy averages, so

$$\overline{\mathbf{B}}(z, t) = \int \mathbf{B}(x, y, z, t) \, dx \, dy / L_x L_y, \tag{2.7}$$

which implies that

$$\langle B^2 \rangle = \langle \overline{B^2} \rangle + \langle b^2 \rangle. \tag{2.8}$$

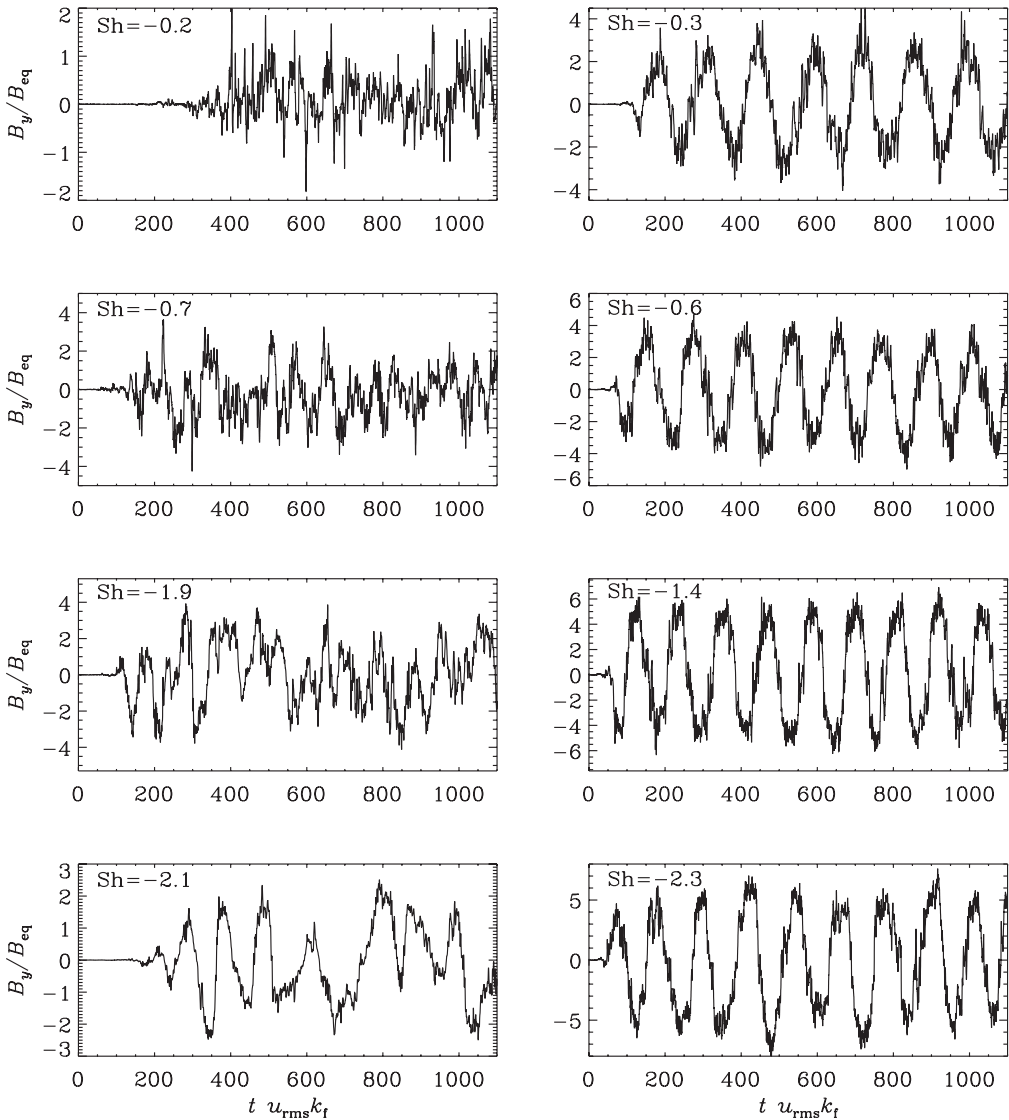


Figure 2. Time series of B_y/B_{eq} for $k_f/k_1 = 1.5$ (left column) and $k_f/k_1 = 2.2$ (right column) for different values of Sh . Again, $Re_M = 22$ for $k_f/k_1 = 1.5$ (left column) and $Re_M = 9$ for $k_f/k_1 = 2.2$ (right column), and $Pr_M = 5$ in both cases. For $k_f/k_1 = 2.2$ the oscillations tend to become less sinusoidal as Sh becomes larger, while for $k_f/k_1 = 1.5$ there are strong fluctuations that tend to become somewhat weaker for larger values of Sh .

One sees that $\langle b^2 \rangle$ shows fluctuations that are not strongly correlated with the variations of the mean field (Figure 1). This is important because the lack of a correlation is sometimes used to argue that the Sun’s small-scale magnetic field must be created by a local small-scale dynamo and disconnected with the large-scale dynamo.

There are several other interesting differences between the two cases. The cycle period is given by $\omega_{cyc} \approx \eta_t k_1^2$ (Käpylä & Brandenburg 2009), and with $\eta_t \approx u_{rms}/3k_f$ (Sur *et al.* 2008) we have $\omega_{cyc} \approx \frac{1}{3}u_{rms}k_f(k_1/k_f)^2$; thus the normalized cycle period is $T_{cyc}u_{rms}k_f \approx 2\pi u_{rms}k_f/\omega_{cyc} \approx 6\pi(k_f/k_1)^2 \approx 91$ for $k_f/k_1 = 2.2$, which agrees with the result shown in

the upper right panel of Figure 1. Next, for $k_f/k_1 = 2.2$ the mean magnetic energy and $\langle \mathbf{B}^2 \rangle$ are about 4 times larger than for $k_f/k_1 = 1.5$. This value is larger than the one expected from the theory where this ratio should be equal to the ratio of the respective values of k_f (Blackman & Brandenburg 2002), namely $2.2/1.5 \approx 1.5$.

Next, we ask how the properties of the dynamo change as it becomes more supercritical. This is shown in Figure 2 where we plot time series of B_y/B_{eq} for $k_f/k_1 = 1.5$ and $k_f/k_1 = 2.2$ for different values of Sh. Note that for $k_f/k_1 = 2.2$ the oscillations become less sinusoidal as Sh becomes larger, while for $k_f/k_1 = 1.5$ there are strong fluctuations that become somewhat weaker for larger values of Sh.

A more quantitative way of assessing the properties of the large-scale dynamo is by looking at the scaling of the magnetic energy of the mean field and the cycle frequency as a function of the nominal dynamo number, $D = C_\alpha C_S$, where

$$C_\alpha = \alpha/\eta_T k_1 = \iota \epsilon_f k_f/k_1, \quad C_S = S/\eta_T k_1 = 3\iota \text{Sh} (k_f/k_1)^2, \quad (2.9)$$

are non-dimensional numbers measuring the expected value of the α effect (assuming $\alpha \approx \frac{1}{3}\tau \langle \boldsymbol{\omega} \cdot \mathbf{u} \rangle$, $\eta_t \approx \frac{1}{3}\tau \langle \mathbf{u}^2 \rangle$, with $\tau = (u_{\text{rms}} k_f)^{-1}$ and $\langle \boldsymbol{\omega} \cdot \mathbf{u} \rangle \approx k_f \langle \mathbf{u}^2 \rangle$), as well as the shear or Ω effect. In these approximations, $\eta_T = \eta + \eta_t$ is the expected total magnetic diffusivity and $\iota = (1 + 3/\text{Re}_M)^{-1}$ is a correction factor that takes into account finite conductivity effects resulting from the fact that $\eta_t \neq \eta_T$. The results are shown in Figure 3.

For $k_f/k_1 = 1.5$, the scaling of $\langle \overline{\mathbf{B}^2} \rangle / B_{\text{eq}}^2$ with D suggests that the critical value is between 1 and 2, i.e., somewhat smaller than the theoretical value of 2 (Brandenburg & Subramanian 2005). For $k_f/k_1 = 2.2$ the critical value is < 1 . The cycle frequencies are approximately independent of D , except that for $k_f/k_1 = 1.5$ there is a sharp drop for $D > 10$. Owing to fluctuations, a Fourier spectrum of the time series is not sharp but has a certain width. We determine the quality or width, w_0 , by fitting the spectrum to a Gaussian proportional to $P(\omega) \sim \exp[-(\omega - \omega_0)^2/2w_0^2]$. Also the values of w_0 , shown in the last panel of Figure 3, are approximately independent of D . For $k_f/k_1 = 2.2$, w_0 is substantially smaller than for $k_f/k_1 = 1.5$. This indicates that the cycle period is better defined for larger scale separation ratios.

3. Active regions and their inclination angle

One should expect that the sunspot number depends in a complicated way on the magnetic field strength. If sunspots are indeed relatively shallow phenomena, the field must be locally concentrated to field strengths of up to 3 kG. A candidate for a mechanism that can concentrate mean fields of ~ 300 G, which is about 10% of the local equipartition field strength, is the negative effective magnetic pressure instability (NEMPI). This is a remarkable phenomenon resulting from the suppression of turbulent pressure by a moderately strong large-scale magnetic field. This suppression is stronger than the added magnetic pressure from the mean field itself, so the net effect is a negative one.

The fact that this phenomenon can lead to an instability in a stratified layer was first found in mean-field models (Brandenburg *et al.* 2010, 2012; Käpylä *et al.* 2012), and more recently in DNS (Brandenburg *et al.* 2011). However, NEMPI has not yet been able to explain flux concentration in the direction along the mean magnetic field, i.e., the large-scale structures remain essentially axisymmetric. To discuss the theoretical origin of this, we need to look at the underlying mean-field theory. Similar to the effective magnetic diffusivity in the mean electromotive force, the sum of Reynolds and Maxwell stresses from the small-scale field depends on the mean magnetic field in a way that looks like a Maxwell stress from the mean field, but with renormalized coefficients. The concept

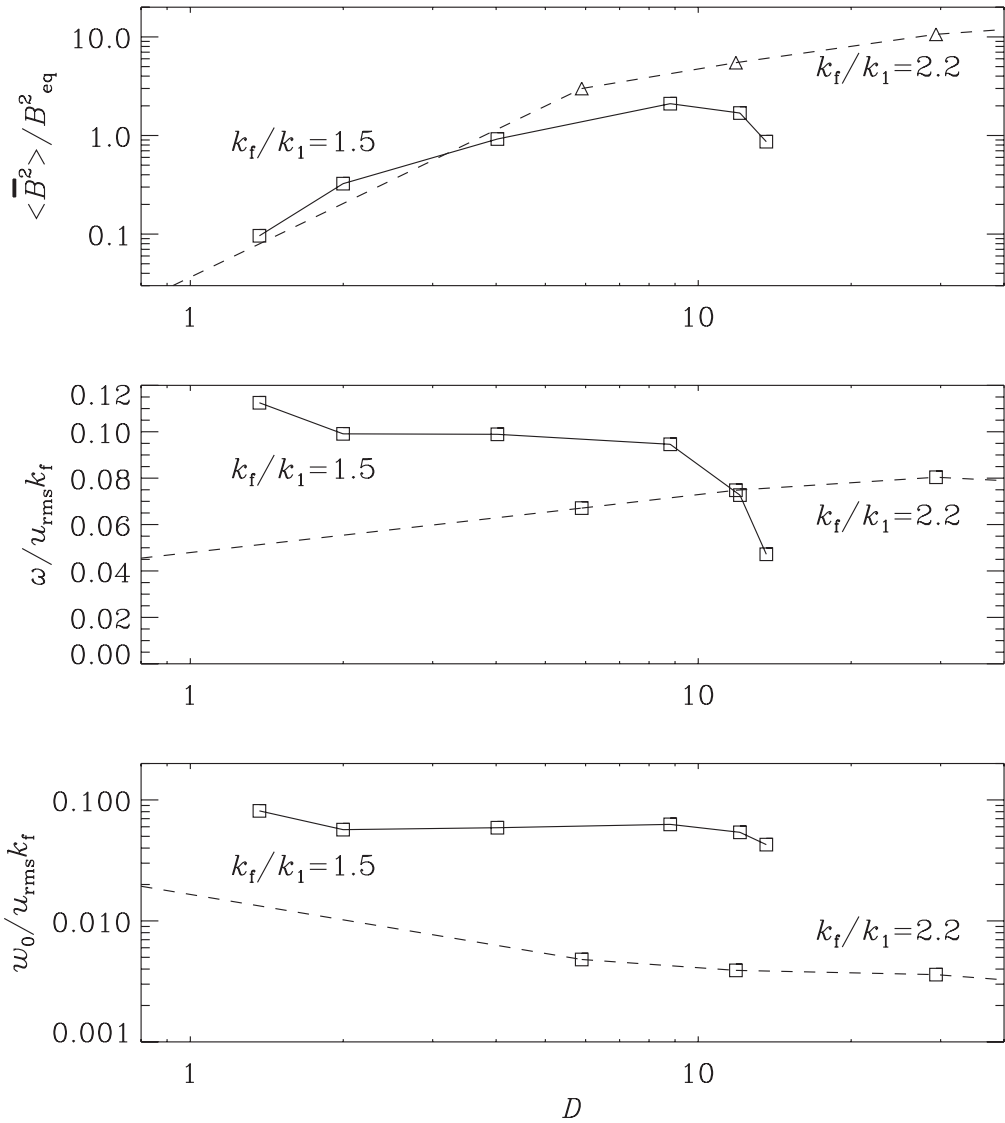


Figure 3. Scaling of the relative magnetic energy of the mean field, $\langle \overline{B}^2 \rangle / B_{eq}^2$, normalized cycle frequency, and normalized quality versus dynamo $D = C_\alpha C_S$.

of expressing the Reynolds stress from the fluctuating velocities, $\overline{u_i u_j}$, by the mean flow \overline{U} is of course familiar and leads to the usual turbulent viscosity term, $-\nu_t(\overline{U}_{i,j} + \overline{U}_{j,i})$. However, in the presence of a mean magnetic field, symmetry arguments allow one to write down additional components, in particular those proportional to $\delta_{ij} \overline{B}^2$ and $\overline{B}_i \overline{B}_j$. The sum of Reynolds and Maxwell stresses from the fluctuating velocity and magnetic fields is given by

$$\overline{\Pi}_{ij}^f \equiv \overline{\rho u_i u_j} - \overline{b_i b_j} / \mu_0 + \frac{1}{2} \overline{b^2} / \mu_0, \tag{3.1}$$

where the superscript f indicates contributions from the fluctuating field. Expressing $\overline{\Pi}_{ij}^f$ in terms of the mean field, the leading terms are (Kleeorin *et al.* 1990; Kleeorin &

Rogachevskii 1994; Kleeorin *et al.* 1996; Rogachevskii & Kleeorin 2007)

$$\bar{\Pi}_{ij}^f = q_s \bar{B}_i \bar{B}_j / \mu_0 - \frac{1}{2} q_p \delta_{ij} \bar{B}^2 / \mu_0 + \dots \quad (3.2)$$

where the dots indicate the presence of additional terms that enter when the effects of stratification affect the anisotropy of the turbulence further. Note in particular the definition of the signs of the terms involving the functions $q_s(\bar{\mathbf{B}})$ and $q_p(\bar{\mathbf{B}})$. This becomes obvious when writing down the mean Maxwell stress resulting from both mean and fluctuating fields, i.e.,

$$-\bar{B}_i \bar{B}_j / \mu_0 + \frac{1}{2} \delta_{ij} \bar{B}^2 / \mu_0 + \bar{\Pi}_{ij}^f = -(1 - q_s) \bar{B}_i \bar{B}_j / \mu_0 + \frac{1}{2} (1 - q_p) \delta_{ij} \bar{B}^2 / \mu_0 + \dots \quad (3.3)$$

A broad range of different DNS have now confirmed that q_p is positive for $\text{Re}_M > 1$, but q_s is small and negative. A positive value of q_s (but with large error bars) was originally reported for unstratified turbulence (Brandenburg *et al.* 2010). Later, stratified simulations with isothermal stable stratification (Brandenburg *et al.* 2012) and convectively unstable stratification (Käpylä *et al.* 2012) showed that it is small and negative. Nevertheless, $q_p(\bar{\mathbf{B}})$ is consistently positive provided $\text{Re}_M > 1$ and \bar{B}/B_{eq} is below a certain critical value that is around 0.5. This implies that it is probably not possible to produce flux concentrations stronger than half the equipartition field strength. So, making sunspots with this mechanism alone is maybe unlikely.

The significance of a positive q_s value comes from mean-field simulations with $q_s > 0$ indicating the formation of three-dimensional (non-axisymmetric) flux concentrations (Brandenburg *et al.* 2010). This result was later identified to be a direct consequence of having $q_s > 0$ (Kemel *et al.* 2012). Before making any further conclusions, it is important to assess the effect of other terms that have been neglected. Two of them are related to the vertical stratification, i.e. terms proportional to $g_i g_j$ and $g_i \bar{B}_j + g_j \bar{B}_i$ with \mathbf{g} being gravity. The coefficient of the former term seems to be small (Brandenburg *et al.* 2012; Käpylä *et al.* 2012) and the second only has an effect when there is a vertical imposed field. However, there could be other terms such as $\bar{J}_i \bar{J}_j$ as well as $\bar{J}_i \bar{B}_j$ and $\bar{J}_j \bar{B}_i$ that have not yet been looked at.

Yet another alternative for causing flux concentrations is the suppression of turbulent (convective) heat transport which might even be strong enough to explain the formation of sunspots (Kitchatinov & Mazur 2000). It is conceivable that effects from heat transport become more important near the surface, so that a combination of the negative effective magnetic pressure and the suppression of turbulent heat transport are needed. Another advantage of the latter is that this mechanism works for vertical fields and is isotropic with respect to the horizontal plane, so one should expect the formation of three-dimensional non-axisymmetric structures.

Once a bipolar active region is formed, we must ask ourselves how to explain the observed tilt angle. This question cannot be answered within the framework of NEMPI alone, but it requires a connection with the underlying dynamo. Here, we can refer to the work of Brandenburg (2005) where bipolar regions occur occasionally at the surface of a domain in which shear-driven turbulent dynamo action was found to operate; see Figure 4. The reason for the tilt is here not the Coriolis force, as is usually assumed, but shear; see also Kosovichev & Stenflo (2008). In the simulations of Brandenburg (2005), shear was admittedly rather strong compared with the turbulent velocity, so the effect is exaggerated compared to what we should expect to happen in the Sun. However, even then there are a few other problems. One of them is that the bipolar regions appear usually quite far away from each other (Figure 4). This may not be realistic. On the other hand, it is not clear how to scale this model to the Sun. In this model, the scale

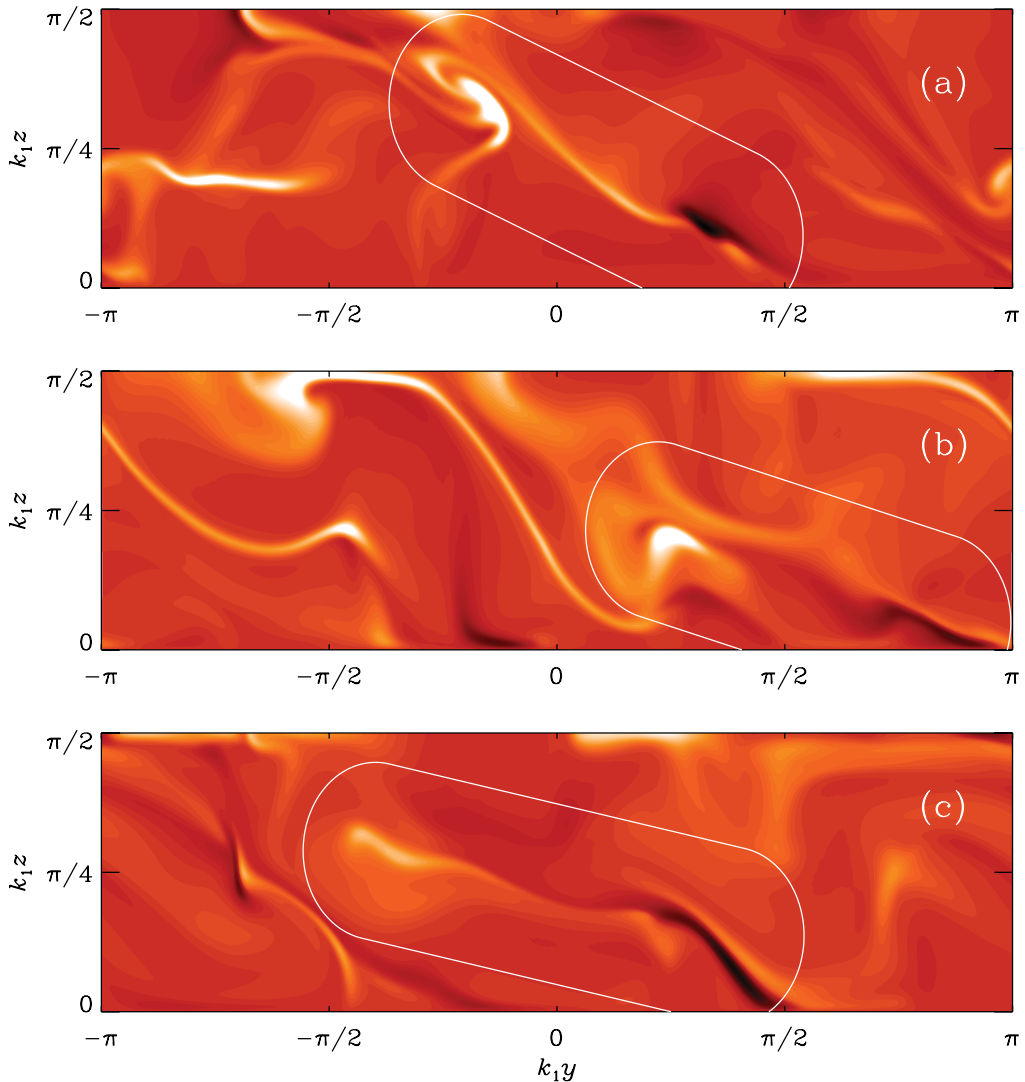


Figure 4. Magnetograms of the radial field at the outer surface on the northern hemisphere at different times for a simulation presented in Brandenburg (2005). Light shades correspond to field vectors pointing out of the domain, and dark shades correspond to vectors pointing into the domain. The elongated rings highlight the positions of bipolar regions. Note the clockwise tilt relative to the y (or toroidal) direction, and the systematic sequence of polarities (white left and dark right) corresponding to $\overline{B}_y > 0$. Here, the z direction corresponds to latitude.

separation ratio is rather small, so the extent of the bipolar regions is comparable to a few times the convective eddy size, which, for the solar surface, is not very big (a few Mm). However, on that small scale one would not expect the effects of differential shear to be very important.

Another issue is that in the model of Brandenburg (2005), bipolar regions occur only occasionally. To illustrate this, we show in Figure 5 the resulting magnetograms for three times that are separated by about 2 turnover times. Clearly, other structures can appear too and the field is not always bipolar.

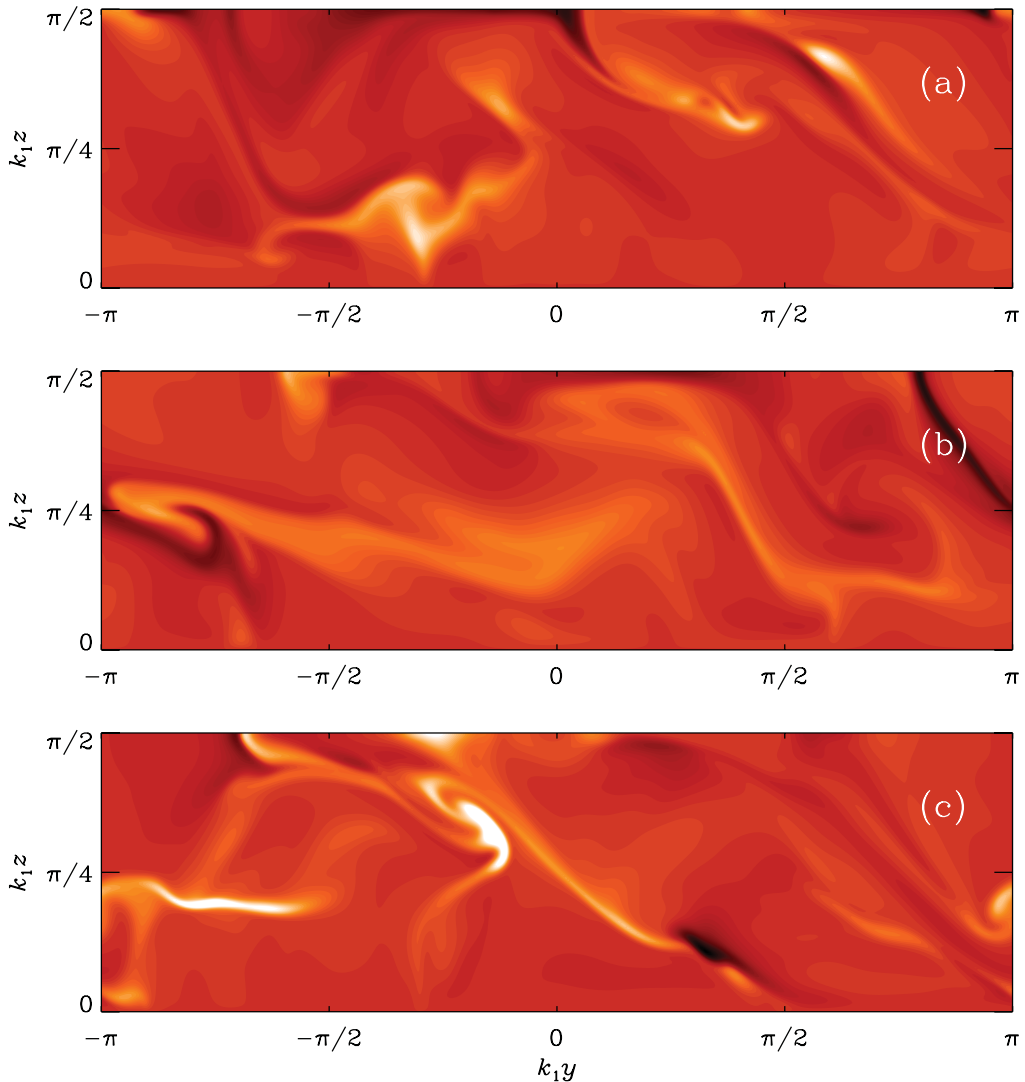


Figure 5. Similar to Figure 4a, showing also the results 4 and 2 turnover times earlier. The last panel is identical to Figure 4a.

4. Conclusions

It is clear that the magnetohydrodynamics of mean magnetic and velocity fields is quite rich and full of important effects. The standard idea that sunspots and bipolar regions form as a result of an instability in the tachocline (Gilman & Dikpati 2000; Cally *et al.* 2003; Parfrey & Menou 2007) may need to be re-examined in view of several new alternative proposals being on the horizon. In addition to comparing models with observations at the solar surface, there are ways of comparison both beneath the surface and above. Particularly exciting are the recent determinations of Ilonidis *et al.* (2011) of some sort of activity at ≈ 60 Mm depth. It is also of interest to explain magnetic activity in the solar wind, and especially its magnetic helicity which has recently been found to be bi-helical, i.e., of opposite signs at large and small length scales (Brandenburg *et al.* 2011) and positive at small length scales in the north. This is particularly interesting,

because such a result has recently been reproduced by distributed dynamo simulations of Warnecke *et al.* (2011) who also find positive magnetic helicity at small length scales in the north. More detailed and varied comparisons between the different approaches are thus required to fully understand the Sun's activity cycles and their long term variations.

Acknowledgments

We acknowledge the allocation of computing resources provided by the Swedish National Allocations Committee at the Center for Parallel Computers at the Royal Institute of Technology in Stockholm and the National Supercomputer Centers in Linköping. This work was supported in part by the European Research Council under the AstroDyn Research Project 227952 and the Swedish Research Council grant 621-2007-4064.

References

- Blackman, E. G. & Brandenburg, A. 2002, *ApJ*, 579, 359
- Brandenburg, A. 2005, *ApJ*, 625, 539
- Brandenburg, A. & Käpylä, P. J. 2007, *New J. Phys.*, 9, 305, 1
- Brandenburg, A., Kemel, K., Kleorin, N., Mitra, D., & Rogachevskii, I. 2011, *ApJ*, 740, L50
- Brandenburg, A., Kemel, K., Kleorin, N., & Rogachevskii, I. 2012, *ApJ*, 749, 179
- Brandenburg, A., Kleorin, N., & Rogachevskii, I. 2010, *Astron. Nachr.*, 331, 5
- Brandenburg, A., Rädler, K.-H., & Kemel, K. 2012, *A&A*, 539, A35
- Brandenburg, A., Rädler, K.-H., Rheinhardt, M., & Käpylä, P. J. 2008, *ApJ*, 676, 740
- Brandenburg, A. & Spiegel, E. A. 2008, *Astron. Nachr.*, 329, 351
- Brandenburg, A. & Subramanian, K. 2005, *Phys. Rep.*, 417, 1
- Brandenburg, A., Subramanian, K., Balogh, A., & Goldstein, M. L. 2011, *ApJ*, 734, 9
- Cally, P. S., Dikpati, M., & Gilman, P. A. 2003, *ApJ*, 582, 1190
- Chatterjee, P. & Choudhuri, A. R. 2006, *Solar Phys.*, 239, 29
- Choudhuri, A. R. 1992, *A&A*, 253, 277
- Choudhuri, A. R., Schüssler, M., & Dikpati, M. 1995, *A&A*, 303, L29
- Dikpati, M. & Charbonneau, P. 1999, *ApJ*, 518, 508
- D'Silva, S. & Choudhuri, A. R. 1993, *A&A*, 272, 621
- Gilman, P. A. & Dikpati, M. 2000, *ApJ*, 528, 552
- Guerrero, G. & de Gouveia Dal Pino, E. M. 2008, *A&A*, 485, 267
- Ionidis, S., Zhao, J., & Kosovichev, A. 2011, *Science*, 333, 993
- Käpylä, P. J., Brandenburg, A., Kleorin, N., Mantere, M. J., & Rogachevskii, I. 2012, *MNRAS*, 2465
- Käpylä, P. J. & Brandenburg, A. 2009, *ApJ*, 699, 1059
- Kemel, K., Brandenburg, A., Kleorin, N., & Rogachevskii, I. 2012, *Astron. Nachr.*, 333, 95
- Kitchatinov, L. L. & Mazur, M. V. 2000, *Solar Phys.*, 191, 325
- Kleorin, N., Mond, M., & Rogachevskii, I. 1996, *A&A*, 307, 293
- Kleorin, N. & Rogachevskii, I. 1994, *Phys. Rev. E*, 50, 2716
- Kleorin, N. I., Rogachevskii, I. V., & Ruzmaikin, A. A. 1990, *Sov. Phys. JETP*, 70, 878
- Kosovichev, A. G., & Stenflo, J. O. 2008, *ApJ*, 688, L115
- Moss, D., Brandenburg, A., Tavakol, R. K., & Tuominen, I. 1992, *A&A*, 265, 843
- Nandy, D., Muñoz-Jaramillo, A., & Martens, P. C. H. 2011, *Nature*, 471, 80
- Parfrey, K. P. & Menou, K. 2007, *ApJ*, 667, L207
- Rogachevskii, I. & Kleorin, N. 2007, *Phys. Rev. E*, 76, 056307
- Ruzmaikin, A. A. 1981, *Comments Astrophys.*, 9, 85
- Schmitt, D., Schüssler, M., & Ferriz-Mas, A. 1996, *A&A*, 311, L1
- Sur, S., Brandenburg, A., & Subramanian, K. 2008, *MNRAS*, 385, L15
- Tavakol, R. K. 1978, *Nature*, 276, 802
- Warnecke, J., Brandenburg, A., & Mitra, D. 2011, *A&A*, 534, A11

Weiss, N. O., Cattaneo, F., Jones, C. A. 1984, *Geophys. Astrophys. Fluid Dyn.*, 30, 305
Yoshimura, H. 1972, *ApJ*, 178, 863

Discussion

ANDRÉS MUÑOZ-JARAMILLO: If sunspots are produced at the surface, which processes would lead to their decay?

AXEL BRANDENBURG: I think it could be the continued submersion of magnetic structures. The system remains time-dependent and new structures will form near the surface, while old ones disappear from view.

JANET LUHMANN: Axel, you are one of the few dynamo modelers that include the corona and larger heliosphere in your models and thinking. How important is that to the results of the models, and do models not including that aspect have compromised results?

AXEL BRANDENBURG: The magnetic helicity flux divergence is crucial for alleviating catastrophic alpha quenching; see the next talk by Candaleresi *et al.* (2011). Helicity fluxes through surface carry about 30% of the total; the rest goes through the equator. The observed magnetic helicity spectra support our understanding in terms of the magnetic helicity evolution equation. Models not including helicity fluxes suffer artificially strong catastrophic quenching, but only if their magnetic Reynolds numbers are really large and magnetic helicity evolution is actually included, which is often not the case either.

ARNAB CHOUDHURI: Flux rise simulations based on the idea that the toroidal field forms in the tachocline explained Joy's law other characteristics of sunspot graphs. Can these results be recovered if sunspots form from near-surface fields?

AXEL BRANDENBURG: The tilt angles of near-surface produced flux concentrations is determined by latitudinal shear, as was demonstrated by Brandenburg (2005). Models with the same shear, but different helicity, give still the same tilt angles

DIBYENDU NANDY: For the near-surface shallow dynamo to work, you need processes that are slow enough to store, amplify, and transport fields on 11 year timescales. However, in the upper convection zone, eddy turnover timescales are short. Can you comment on how you reconcile this with your shallow dynamo?

AXEL BRANDENBURG: Magnetic helicity conservation is generally responsible for prolonging the time scales. In fact, the partial alleviation of catastrophic quenching by magnetic helicity fluxes means that the timescales are not infinite. The dynamo period is proportional to $(\alpha\partial\Omega/\partial r)^{-1/2}$, so α quenching prolongs the period. As far as active region formation by NEMPI is concerned, the relevant time scale was shown to be longer than the eddy turnover time by a factor that is equal to the square of the scale separation ratio (Brandenburg *et al.* 2011).